J Mater Sci (2012) 47:7841–7847
DOI 10.1007/s10853-012-6661-2

ULTRAFINE GRAINED MATERIALS

Evolution of ultrafine microstructures in commercial purity aluminum heavily deformed by torsion

Sunisa Khamsuk · Nokeun Park · Hiroki Adachi · Daisuke Terada · Nobuhiro Tsuji

Received: 8 March 2012 / Accepted: 10 June 2012 / Published online: 28 June 2012

Abstract Commercial purity aluminum (1100Al) bars were severely plastic deformed by torsion deformation at room temperature. The specimens were deformed to ultrahigh equivalent strain of 5.85 in maximum. Microstructure evolution during the torsion deformation was characterized using electron back scatter diffraction analysis on two different sections: the longitudinal section parallel to the torsion axis and transverse section perpendicular to the torsion axis. The grain size decreased and the fraction of high angle grain boundary increased with increasing equivalent strain. Elongated ultrafine grained structure was obtained after an equivalent strain of 3.27. We have found that the microstructure evolution in the specimen deformed by torsion exhibited similar behavior to those in the same material heavily deformed by accumulative roll bonding. The average grain size of 0.32 μm with the high angle boundary fraction of 0.76 was achieved in the specimen deformed to an equivalent strain of 5.27. Though the microstructure and hardness on the transverse section varied depending on the radial positions, they could be arranged as a simple function of equivalent strain. The present work confirmed that the torsion deformation worked as a kind of severe plastic deformation.

S. Khamsuk · N. Park · D. Terada · N. Tsuji (✉)
Department of Materials Science and Engineering,
Kyoto University, Yoshida-honmachi, Sakyo-ku,
Kyoto 606-8501, Japan
e-mail: nobuhiro-tsuji@mtl.kyoto-u.ac.jp

H. Adachi
Department of Materials Science and Chemistry,
Graduate School of Engineering, University of Hyogo, Himeji,
Hyogo 671-2280, Japan

Introduction

Severe plastic deformation (SPD) has been successfully used for producing bulk ultrafine grained metallic materials with grain sizes smaller than 1 μm [1]. Several SPD techniques are now available for introducing high strains into bulk materials including cyclic extrusion compression (CEC) [2], high pressure torsion (HPT) [3], equal channel angular pressing (ECAP) [4, 5], and accumulative roll bonding (ARB) [6]. It has been known that the formation process of ultrafine grained structures can be understood in terms of *grain subdivision* [7–11], where deformation induced boundaries subdivide the original crystals [10, 11]. It has been also known that a certain amount of strain is necessary to obtain ultrafine grains with large misorientations [12]. On the other hand, the effects of other deformation conditions, i.e., strain rate and temperature, on the formation of ultrafine structures have not yet been systematically understood. This is primarily because most of the SPD processes mentioned above are the discontinuous "batch" processes in which it is difficult to carry out ultrahigh strain deformation at a constant strain rate and temperature continuously. On the other hand, torsion deformation could be a kind of SPD method in which strain rate and temperature are controlled more effectively. Although torsion deformation has often been used to simulate thermomechanical processing such as multi-pass barrolling [13, 14], this process has been rarely used for production of bulk ultrafine grained materials. In addition, the change in microstructure and mechanical properties of ultrafine grained materials fabricated by torsion deformation process has not been clarified yet. On this background, the present work aims to clarify the change in microstructure and mechanical properties of a commercial purity aluminum in torsion deformation at ambient temperature.

Experimental

Commercial purity aluminum (1100Al) bars 8 mm in diameter were prepared for this study. The chemical composition of the material is shown in Table 1. The starting bars had a fully recrystallized microstructure with an average grain size of 23 μm. The starting bars were machined into torsion specimens with dimensions of 4 mm in gage length and 8 mm in diameter (Fig. 1a), and torsion deformation was applied to achieve high strain deformation. The specimens were deformed in torsion at room temperature by rotations of 0.25, 0.5, 1.0, 1.5, and 1.60, corresponding to the maximum equivalent strains of 0.91, 1.81, 3.63, 5.44, and 5.85 at the specimen surface, respectively. The equivalent strain in torsion can be calculated by following equations [15]:

$$\gamma = \frac{2\pi Nr}{L} \tag{1}$$

$$\varepsilon_{eq} = \frac{\gamma}{\sqrt{3}} \tag{2}$$

where ε_{eq} is equivalent strain, γ shear strain, N the number of rotation, r the radial position in the specimen, and L the gauge length of the specimen. The rotation speed in torsion was 1.66×10^{-5} rpm so that the strain rate at the specimen surface was 10^{-3} s^{-1}.

Microstructures of the torsion deformed specimens were characterized by electron backscatter diffraction (EBSD). The EBSD scans were carried out on the longitudinal section at $r = 0.9R$ (R: radius of the specimen) position from the center of the specimen (Fig. 1b) and at different locations on the transverse sections perpendicular to the torsion axis to examine the structure heterogeneity (Fig. 1c). Specimens for EBSD analysis were prepared by electropolishing at −30 °C at a voltage of 12 V in a solution of 300 ml HNO_3 + 700 ml CH_3OH. EBSD observation was carried out in a field-emission type scanning electron microscope (FE-SEM), model FEI (Phillips) Siron, at an accelerating voltage of 15 kV.

Hardness tests were conducted for the torsion deformed specimens using Shimadzu micro-hardness tester equipped with Vickers indenter. Load of 1 kg with dwell time of 10 s was used in all tests. Hardness measurements were carried out at various radial positions on the polished surfaces of transverse sections of the torsion specimens, as is shown schematically in Fig. 1c.

Table 1 Chemical composition of the 1100Al studied (mass%)

Si	Fe	Cu	Mn	Zn	Ti	Al
0.09	0.61	0.11	0.01	0.02	0.02	Bal.

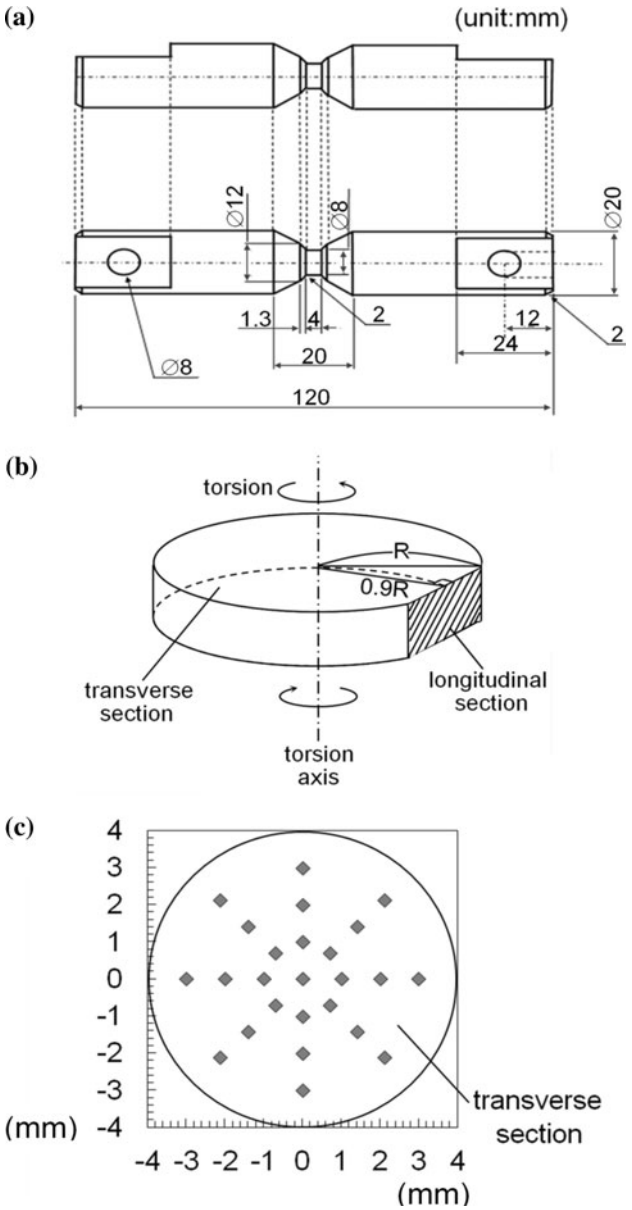

Fig. 1 Schematic illustrations of **a** the torsion specimen, **b** the longitudinal section for EBSD, and **c** the positions of hardness measurement on the transverse section

Results and discussion

Microstructure evolution during torsion deformation

Figure 2 shows grain boundary maps obtained from the EBSD measurements on longitudinal sections of the starting material and the specimens torsion deformed to various equivalent strains (ε_{eq} = 0.82–5.27), where these equivalent strains were calculated at the observed regions (0.9R). In the figure, the black and gray lines represent high angle grain boundaries ($\theta \geq 15°$, θ: misorientation) and low angle grain boundaries ($2 \leq \theta < 15°$), respectively. Boundaries with

misorientation below 2° are not included in the figure due to the uncertainty in EBSD measurement and analysis. It is clearly seen in Fig. 2a that the starting material exhibits a fully recrystallized microstructure with the average grain size of 23 μm. In cases of the imposed equivalent strains below 2, low angle boundaries are mainly observed along the shear direction (Fig. 2b, c). With increasing torsion strain, fine grains surrounded by high angle grain boundaries are generated. However, a large number of (sub)grains with low angle boundaries remain in the structure after $\varepsilon_{eq} = 3.27$ (Fig. 2d). By increasing equivalent strain to 4.90, the amount of fine grains with high angle boundaries are increased (Fig. 2e). The specimen deformed to an equivalent strain of 5.27 exhibited finer and more equiaxed grains. When all boundaries are taken into account, the mean grain size was 0.32 μm. Most of those fine grains are surrounded by high angle grain boundaries (Fig. 2f).

The average (sub)grain size and fraction of high angle boundaries obtained from the EBSD data are summarized in Table 2, where D_{All} is the average (sub)grain size obtained from all boundaries having misorientation above 2° and D_{HAGB} is the mean grain size obtained from high angle grain boundaries ($\theta \geq 15°$). Fractions of high angle boundaries are also summarized in the table. The main finding is the evolution of ultrafine grained microstructure in the 1100Al with increasing torsion strain. The grain size decreases and the fraction of high angle grain boundaries increases with increasing equivalent strain. Similar observations have been reported in several materials severely deformed by ARB [16], ECAP [4, 17], and HPT [18, 19] processes. It has been considered that the formation of ultrafine grained microstructures during high plastic deformation can be understood in terms of *grain subdivision*. *Grain subdivision* [10, 11] is the process in which geometrically necessary boundaries (GNBs) induced by plastic deformation subdivide the original crystals. Based on the microstructural results, the features of the ultrafine

Table 2 Summary of the microstructural parameters in the 1100Al specimens torsion deformed to various equivalent strains, where D_{All} is the average (sub)grain size with misorientation above 2°, D_{HAGB} is the mean grain size obtained from high angle grain boundaries ($\theta \geq 15°$)

Equivalent strain (at 0.9*R*)	Average grain size (μm)		Fraction of high angle boundaries, F^{HAGB}
	D_{All}	D_{HAGB}	
0	23.4	28.0	0.76
0.82	1.94	6.29	0.18
1.63	0.56	1.86	0.35
3.27	0.40	0.46	0.55
4.90	0.35	0.36	0.67
5.27	0.32	0.33	0.76

The parameters were measured using EBSD data on longitudinal sections like Fig. 1

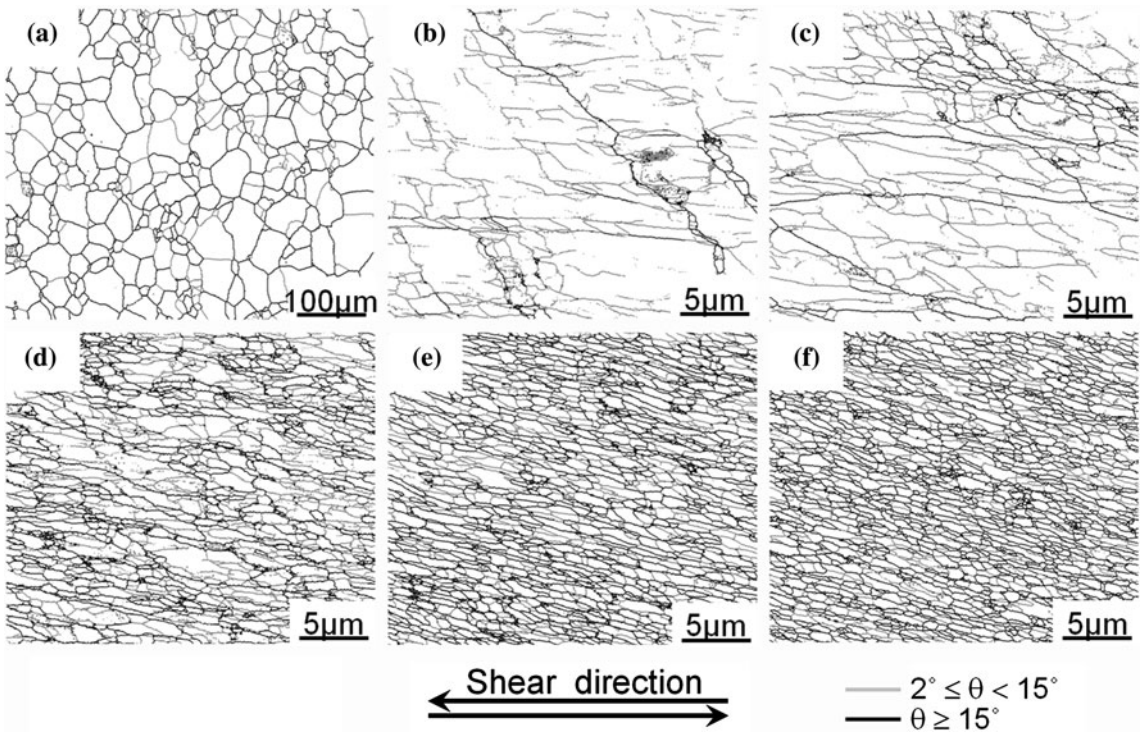

Fig. 2 EBSD boundary maps of the specimens torsion deformed to various equivalent strains. **a** Undeformed material, **b** $\varepsilon_{eq} = 0.82$, **c** $\varepsilon_{eq} = 1.63$, **d** $\varepsilon_{eq} = 3.27$, **e** $\varepsilon_{eq} = 4.90$, and **f** $\varepsilon_{eq} = 5.27$. Observed on the longitudinal sections at 0.9*R*

grain formation during torsion deformation process can be described as follows: at low strain ($\varepsilon_{eq} < 2$), the original grains are deformed and start to be subdivided into subgrains with low angle misorientation, and those subgrains are elongated in the direction nearly parallel to the shear direction, as shown in Fig. 2b, c. New ultrafine grains with high angle boundaries are generated at medium strains ($\varepsilon_{eq} < 4$). At this stage a number of low angle boundaries still remain in the structure as shown in Fig. 2d. An ultrafine grain structure with the fraction of high angle grain boundaries above 0.65 was obtained at high strains ($\varepsilon_{eq} \geq 4.9$). Equiaxed ultrafine grains ($\sim$0.32 μm) are formed homogeneously in the microstructure at ultrahigh strain ($\varepsilon_{eq} = 5.27$) as seen in Fig. 2f. Our results agree well with that by Hansen et al. [10] who demonstrated that elongated deformation structures of pure aluminum formed by conventional rolling transformed from oriented structures into an equiaxed structures at high strain. Indication of such transition has been also observed in the processes where deformation involves a significant shear component [10], and when the deformation direction is changed [11].

Comparison between torsion deformation and ARB

Figure 3 shows a comparison between torsion deformation and ARB process by plotting the average grain size (D_{All}) and fraction of high angle boundaries in the 1100Al deformed by both processes as a function of equivalent strain. The ARB data were taken from a previous report by Kamikawa [20]. It is obvious in Fig. 3a that the grain size of the specimens deformed by torsion exhibits the same trend as those deformed by ARB. Grain size decreases with increasing strain. However, observing the microstructural change in Fig. 3a carefully (see the inset), it is found that at similar strains the grain sizes of the ARB processed specimens are finer than those in the torsion deformed specimen. At the same time, it was also observed that the increasing rate of misorientation in the ARB processed specimens is greater than that in the torsion deformed specimens. In other words, the evolution of the ultrafine grained structures in the 1100Al was faster in the ARB than in the torsion. Probably this difference is caused by the difference in strain path. In the torsion deformation, monotonic simple shear is the dominant deformation mode, while the deformation in the ARB process is more complicated. Because the corresponding ARB process was carried out without lubrication [20], redundant shear strains were applied at the subsurface regions of the sheet due to large friction between rolls and the sheet, in addition to the plane strain compression by normal rolling. Half of the surface regions come to the center in the ARB process, making the strain path of each region complicated. A similar observation has been reported by Zhilyaev et al.

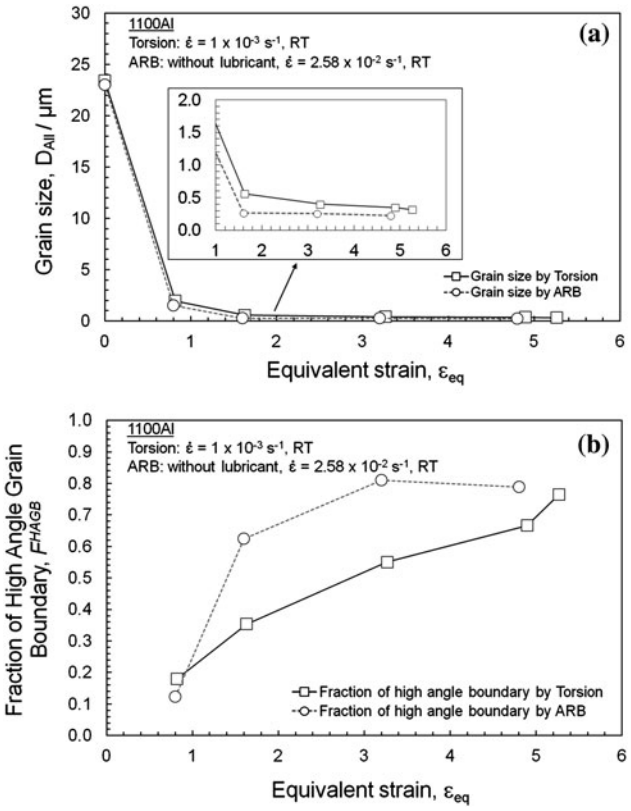

Fig. 3 **a** Average grain size (D_{All}) and **b** fraction of high angle boundaries (F^{HAGB}) in the 1100Al deformed by torsion or ARB [20], plotted as a function of equivalent strain

[21] who demonstrated that different deformation processes resulted in different grain sizes in a high purity nickel.

Microhardness

Figure 4 shows the hardness values at various radial positions in the torsion specimens after different rotation from 0.5 to 1.60. The hardness measurements were carried out on the transverse sections perpendicular to the torsion axis, as was shown in Fig. 1. The lower broken line corresponds to the hardness level of the unprocessed specimen, 27.4 Hv. The main results presented in Fig. 4 are summarized as follows. First, the hardness values increase with increasing applied torsion rotation. Second, the values of hardness increase with increasing the distance from the center of the specimen. This is attributed to difference in strain along the radial position in torsion deformation, as is expressed in Eq. (1). According to Eq. (1), the shear strain at the center is ideally zero and it increases linearly with approaching to the surface. Thus, the microstructure along the radius should be inhomogeneous, as is shown later. The hardness value near the center reveals strain hardening, although the strain at the centre should be ideally zero. This

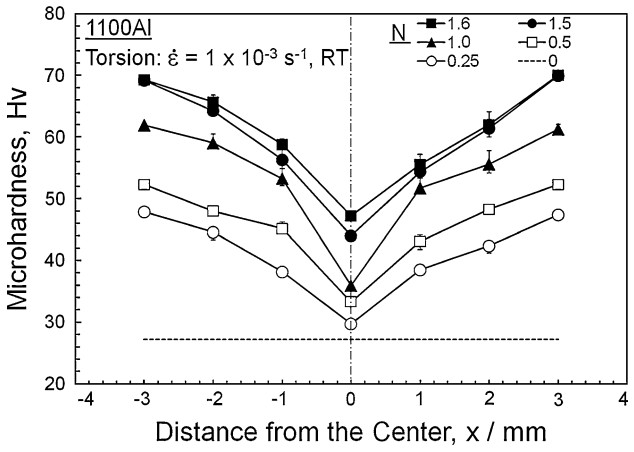

Fig. 4 Average microhardness values at various radial positions in the 1100Al specimens torsion deformed to different rotations (*N*)

may be attributed to compressive deformation happening in the torsion process. The increase of the hardness with plastic strain is caused by strain hardening and grain refinement strengthening.

Figure 5 shows the EBSD grain boundary maps at different radial positions in the 1100Al specimen torsion deformed by 1.5 rotations: (a) at the center of the sample ($r = 0$), (b) $r = 0.2R$, (c) $r = 0.5R$, and (d) $r = 0.9R$. Corresponding equivalent strains are 0, 1.09, 2.72, and 4.90, respectively. The results clearly show that these four areas have different microstructures. The microstructure at the center of the sample, where the shear strain should be ideally zero, shows coarse grains with a few low angle boundaries (Fig. 5a). In Fig. 5b, new grains with smaller grain sizes are partly formed, but most of the regions are composed of low angle boundaries (deformation

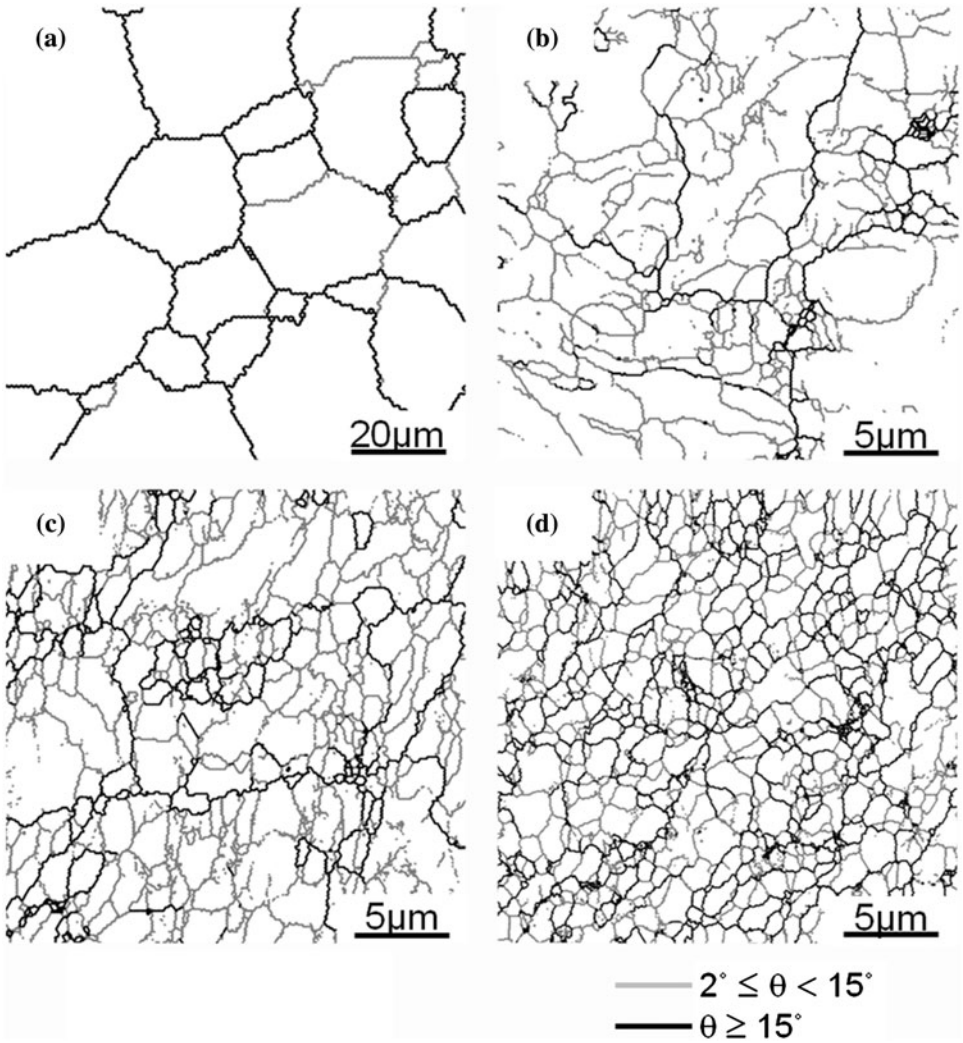

Fig. 5 EBSD grain boundary maps at different radial positions of the 1100Al specimens torsion deformed by 1.5 rotations. **a** At the center of the sample ($r = 0$), **b** $r = 0.2R$, **c** $r = 0.5R$, and **d** $r = 0.9R$, where R is the radius of the sample (4.0 mm). The corresponding equivalent strains (ε_{eq}) are **a** 0, **b** 1.09, **c** 2.72, and **d** 4.90, respectively

structures). Grain size decreases with increasing the distance from the center to the edge of the specimen, i.e., with increasing equivalent strain (Fig. 5c, d). The mean grain sizes (D_{All}) at different positions from 0 to 0.9R are 17.2, 2.0, 0.99, and 0.62 μm, respectively. The fractions of high angle boundaries at 0–0.9R are 0.85, 0.18, 0.30 and 0.53. The fraction of high angle boundaries rapidly decreases from the center to 0.2R (Fig. 5b), and then it increases significantly with increasing distance from the specimen axis.

It was found that at the same strain the fraction of high angle boundary observed from the transverse section (Fig. 5) was lower than those observed on longitudinal section (Fig. 3b). The discrepancy might be attributed to the difference in strain rate along the radial position in torsion deformation. The strain and strain rate increase with approaching to the edge of the specimen, so that the microstructures observed on the transverse section were those formed under lower strain rate even at the same level of strain. On the other hand, it should be noted that even at the same edge position (0.9R), the grain size observed on the transverse section was smaller than that observed on the longitudinal section. This indicates that three-dimensional morphology of the ultrafine grains formed by torsion is not equiaxed.

The hardness data in Fig. 4 are replotted as a function of equivalent strain in Fig. 6. It can be seen that the hardness continuously increases with increasing equivalent strain, which means that the hardness corresponds well with the plastic strain imposed. We also found the scattering of hardness values at the center regions; the hardness value obviously increases with increasing deformation rotation. By the way, a homogeneous microstructure has been reported in Al processed to high strain by HPT [22]. The deformation in HPT is fundamentally similar to the torsion deformation, i.e., monotonic simple shear. This difference is presumably attributed to the fact that the previous study in HPT was carried out up to extremely high shear strain of 184, which corresponds to total equivalent strain of 106. At the same time, there are several reports showing inhomogeneous hardness distribution after HPT process [23–25]. Vorhauer and Pippan [25] have found that an inhomogeneous microstructure appeared in an austenitic steel deformed to ultrahigh strain ($\varepsilon_{eq} = 324$) by HPT [25]. This difference may suggest that the strain necessary for obtaining homogeneous microstructure depends on the kind of materials.

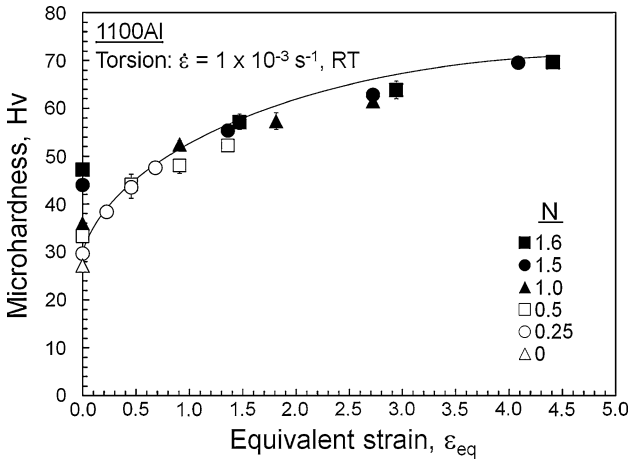

Fig. 6 Average microhardness values at various radial positions of the 1100Al specimens deformed to different torsion rotations (N), plotted as a function of equivalent strain

It can be concluded from the present investigation that torsion deformation works as a kind of SPD for fabricating ultrafine grained microstructures. Although the microstructures were heterogeneous depending on the radial positions, the microstructural parameters were well understood in terms of equivalent strain. The results indicate that torsion deformation is useful to investigate the effect of deformation conditions on the ultrafine grain formation, which will be studied in our following studies.

Conclusions

In this work, the effect of strain on microstructure and hardness of commercial purity 1100 aluminum deformed by torsion deformation has been studied. The main results are summarized as follows;

(1) The grain size decreased and fraction of high angle boundaries increased with increasing plastic strain in torsion deformation. The grain size of 0.32 μm and the high angle boundary fraction of 0.76 were achieved after equivalent strain of 5.27. It can be concluded that the torsion deformation worked as a kind of SPD. The torsion would make it possible to study ultrahigh strain deformation under controlled temperature and strain rate.

(2) The grain size and misorientation angle of the 1100 aluminum deformed by torsion had the same trend as those heavily deformed by ARB. However, the ARB process showed higher efficiency in producing ultrafine grained microstructure than torsion deformation. This was probably because the strain path in torsion was much simpler than that in ARB.

(3) The hardness values increased with increasing the equivalent strain and the radial position in the sample. Although the hardness and microstructure were heterogeneous on the transverse sections, they showed a good correlation with the equivalent strain imposed.

Acknowledgements This study was financially supported by the Grant-in-Aid for Scientific Research on Innovative Area, "Bulk Nanostructured Metals", from the Ministry of Education, Culture, Sports, Science and Technology of Japan, and the support is gratefully acknowledged.

References

1. Segal V (2006) In: Altan BS (ed) Severe plastic deformation: towards bulk production of nanostructured materials. Nova science publishers, New York, p 1
2. Richert M, Liu Q, Hansen N (1999) Mater Sci Eng A 260:275
3. Zhilyaev A, Langdon T (2008) Prog Mater Sci 53:893
4. Segal V (1999) Mater Sci Eng A 271:322
5. Valiev R, Langdon T (2006) Prog Mater Sci 51:881
6. Tsuji N, Saito Y, Lee SH, Minamino Y (2003) Adv Eng Mater 5:338. doi:10.1002/adem200310077
7. Huang X, Tsuji N, Hansen N, Minamino Y (2003) Mater Sci Eng A 340:265
8. Terada D, Inoue S, Tsuji N (2007) J Mater Sci 42:1673. doi:10.1007/s10853-006-0909-7
9. Hughes D, Hansen N (1997) Acta Mater 45:3871
10. Hansen N, Jensen DJ (1999) Philos Trans R Soc Lond Ser A 357:1447
11. Hansen N (2001) Metall Mater Trans A 32:2917
12. Liu Q, Huang X, Lloyd DJ, Hansen N (2002) Acta Mater 50:3789
13. Nakata N, Militzer M (2005) ISIJ Int 45:82
14. Debray B, Teracher P, Jonas JJ (1995) Metall Mater Trans A 26:99
15. Shrivastava SC, Jonas JJ, Canova G (1982) Mech Phys Solids 30:75
16. Hosseini S, Manesh H (2009) Mater Des 30:2911
17. Neishi K, Horita Z, Langdon T (2002) Mater Sci Eng A 325:54
18. Todaka Y, Umemoto M, Yamazaki A, Sasaki J, Tsuchiya K (2008) Mater Trans 49:7
19. Loucif A, Figueiredo RB, Baudin T, Brisset F, Longdon T (2010) Mater Sci Eng A 527:4864
20. Kamikawa N (2005) Grain refinement of structural metallic materials by accumulation roll bonding. PhD thesis, Osaka University
21. Zhilyaeva A, Kim B, Nurislamova G, Baroo M, Szpunar J, Langdon T (2002) Scripta Mater 46:575
22. Xu C, Horita Z, Langdon T (2007) Acta Mater 55:203
23. Jiang H, Zhu Y, Butt D, Alexandrov I, Lowe T (2000) Mater Sci Eng A 290:128
24. Sakai G, Nakamuraa K, Horita Z, Langdon T (2005) Mater Sci Eng A 406:268
25. Vorhauer A, Pippan R (2004) Scripta Mater 51:921